Supplementary material to the article "Single-electron spectrum of a short-period InAs/GaSb superlattice with strain compensation governed by interface layers"

1. Stress compensation and In(As)Sb layers.

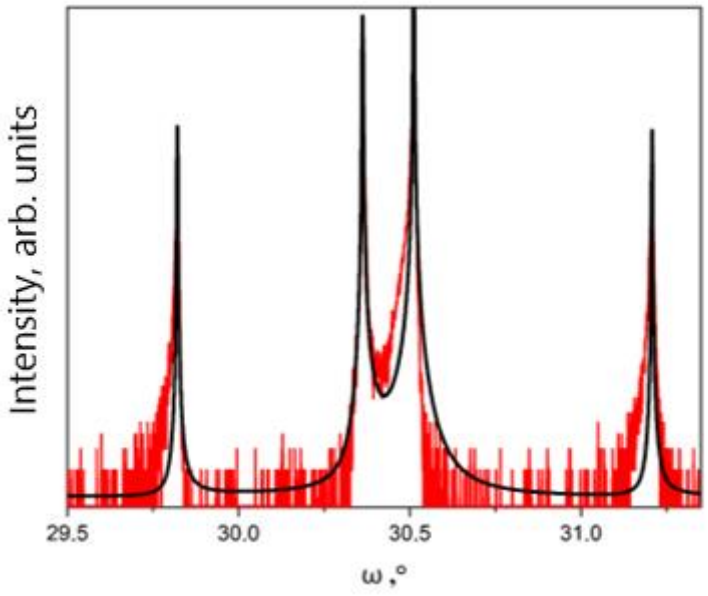

Fig. S1. X-ray rocking curve of a SL containing 300 periods near the (004) reflection (red curve). The black curve is a calculation based on the nominally specified SL parameters.

The red curve in Fig. S1 illustrates the X-ray rocking curve of a superlattice (SL) containing 300 periods. The thicknesses of the InAs and GaSb layers are 5 nm and 2.5 nm, respectively. As can be seen from the figure, the angular shift of the peak corresponding to the center of gravity of the SR is located in the region of 30.5°, which proves the absence of plastic stress relaxation. The described above SL was obtained using the same interface technological procedure as the 100-period SL being discussed in the article.

During the growth of an epitaxial InAs layer (lattice constant 6.06 nm) on GaSb (lattice constant 6.038 nm), plastic relaxation, accompanied by the defect formation at the InAs/GaSb interface, is registered at an InAs layer thickness of about 20 nm [1]. This value is qualitatively consistent with the well-known equation for estimating the critical thickness (l_{cr}) of stressed layers if relaxation is governed by perfect 60° dislocations [2]:

$$l_{cr} = \frac{2\,b(1-\nu/4)}{8\pi f(1+\nu)} Ln(\frac{l_{cr}}{b}+1) \qquad \text{(S1)}$$

Where b is the Burgers vector of dislocations, ν is Poisson's ratio, f is a parameter characterizing the mismatch of the lattice constant. For A_3B_5 semiconductor compounds from the "6.1 A" family, $b \sim 0.43$ (InAs), $\nu \sim 0.35$ for the GaSb/InAs pair and $f = 0.0062$. These values make it possible to estimate the critical thickness as $l_{cr} \sim 17$ nm, which is in good agreement with the experimentally measured value.

In the case of SL with an InAs to GaSb thickness ratio of 2:1, it is easy to obtain an estimate for the lattice parameter mismatch of $f \sim 0.003$. Using the above values of b and ν for a rough estimate and using (S1), we obtain the critical SL thickness $l_{cr} \sim 42$ nm. In the case of SL containing 300 periods, the resulting value is approximately 50 times less than the total thickness of the SL. Thus, the absence of relaxation for SL containing 300 periods proves the presence of mechanisms

which compensate elastic stresses. A necessary condition for compensation is the presence of semiconductor layers with a lattice constant greater than that of GaSb. In the InGaAsSb material system, only InSb and $InAs_xSb_{1-x}$ solid solutions with x <0.9 have this property. Thus, the presented experimental data, combined with estimates of the critical thickness, prove the successful introduction of In(As)Sb layers into the superlattice. Those layers, having a thickness of about 1-2 monolayers, are difficult to investigate using direct measurements such as X-ray data or TEM.

2. Calculation of the complex refractive index of a GaSb substrate.

The calculation of the complex refractive index $N = n + i\kappa$ was carried out for two ranges 500-2000 cm^{-1} and 2000-7000 cm^{-1} by different methods using standard Wolfram Mathematica software packages.

2.1. 2000-7000 cm^{-1} range.

n and κ for a substrate without an epitaxial structure were calculated based on the formulas used to calculate the transmittance of a flat plate by summing all the reflected waves. Interference oscillations on the thickness of the plate were averaged, which made it possible to obtain the following expressions:

$$R_e^{Sub} = R_3 + T_3^2 A^2 R_3/(1 - A^2 R_3^2) \quad \text{(S2)}$$

$$T_e^{Sub} = T_3^2 A/(1 - A^2 R_3^2) \quad \text{(S3)}$$

where R_e^{Sub} and T_e^{Sub} are experimental data on the reflection and transmission of the substrate, respectively, and R_3, T_3 and A are related to n and κ by the following relations:

$$R_3 \approx \left|\frac{1-n-i\kappa}{1+n+i\kappa}\right|^2, \quad \text{(S4)}$$

$$T_3 = 1 - R_3, \quad \text{(S5)}$$

$$A = \exp(-\frac{2\cdot 2\pi}{\lambda} n). \quad \text{(S6)}$$

The numerical solution of equations (S2,S3) with respect to n and κ allows us to reconstruct the frequency dependence of the complex refractive index for the range in which data on the transmission of the substrate is available, see Fig. S2.

2.2. 500-2000 cm^{-1} range.

In this range, the experimental measurement of T_e^{Sub} is not available due to the strong absorption of the substrate, however, taking into account that n is three orders of magnitude greater than κ in the range of 2000 cm^{-1} (see Fig. S2), the κ in (S4) can be neglected. In this case, n can be easily calculated using the formula:

$$n \approx \frac{1-\sqrt{R_e^{Sub}}}{1+\sqrt{R_e^{Sub}}} \quad \text{(S7).}$$

The results obtained for n are shown on the left side of Figure S1.

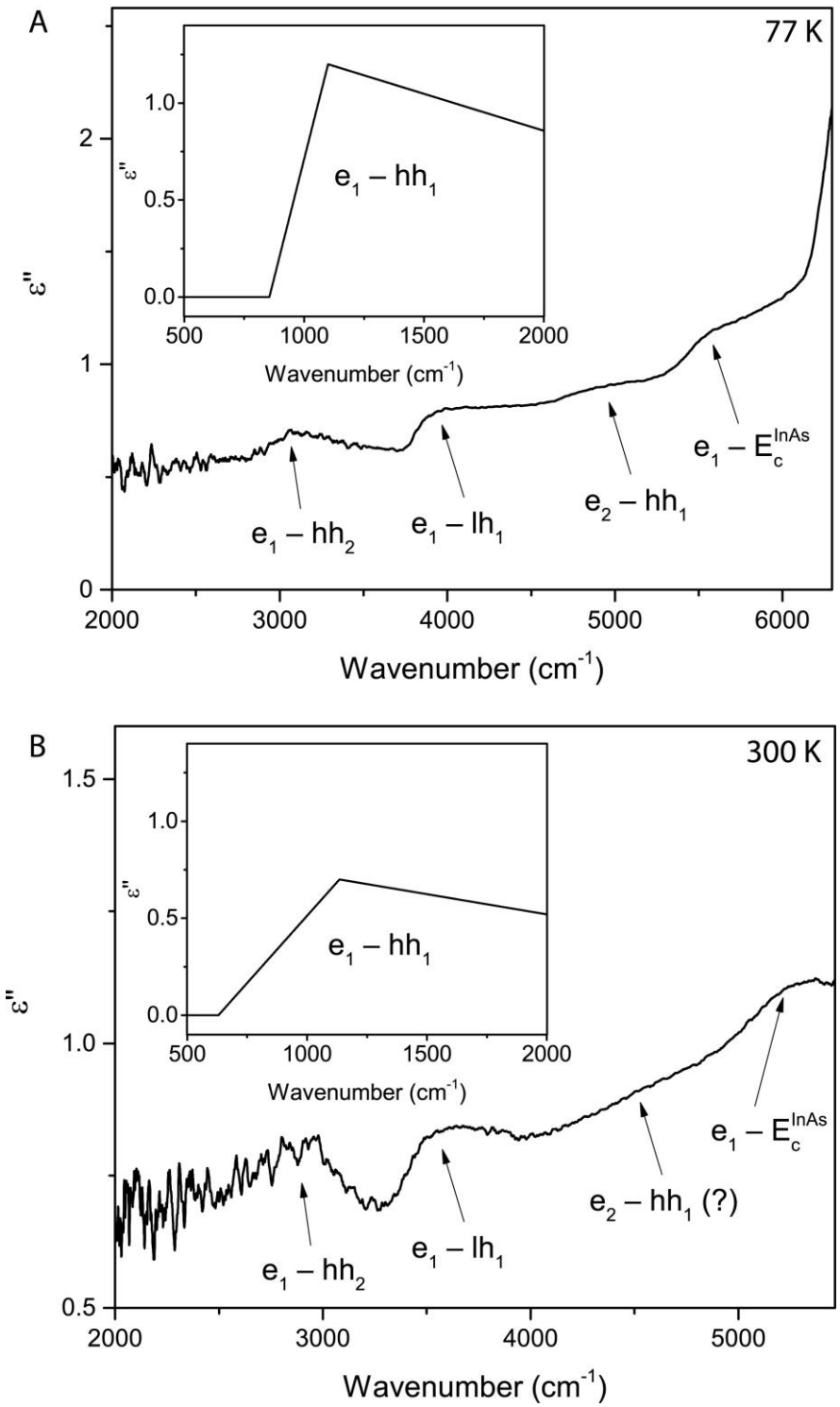

Fig.S2. Frequency dependence of ε" at temperatures 77 K (A) and 300 K (B). The insets show the results of ε'' estimates in the 500-2000 cm^{-1} range.

3. Calculation of the complex refractive index of a SL

Calculation of refractive and absorption indices in SL was carried out for two ranges 500-2000 cm^{-1} and 2000-7000 cm^{-1} by different methods using standard Wolfram Mathematica software packages.

3.1. 2000-7000 cm^{-1} range.

When calculating the refractive index of a SL, it is necessary to take into account the influence of the substrate. Here the consideration is limited to the situation in which the reflected plane electromagnetic wave is directed perpendicular to the surface of the heterostructure containing a SL. This geometry is fully consistent with the experiment that was used to measure the spectral dependence of the reflectance in the IR range.

A diagram of a heterostructure with a wave incident on it (E) and waves arising due to reflection from various boundaries (E_1, E_2, E_3, E_4) are shown in Fig. S3. Let the three media under consideration - the external medium, the SL and the substrate - be characterized, respectively, by complex refractive indices N_1, N_2, N_3. A noticeable portion of the emission transmitted into the substrate is absorbed in it. Part of the electromagnetic emission reflected by the back side of the substrate and returned to the SL/substrate interface leads to the appearance of a rapidly oscillating interference additive. Averaging this addition, associated, for example, with insufficient resolution of the spectrograph, is similar to neglecting the contribution from interference involving a wave reflected from the back side of the substrate.

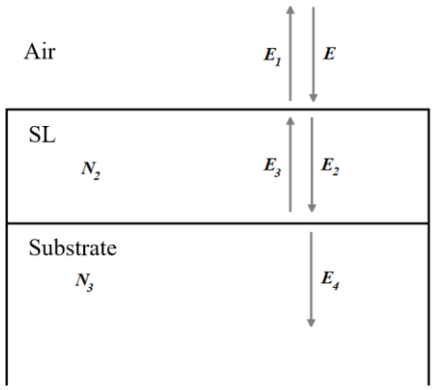

Fig. S3 Diagram of reflection of a plane wave from a heterostructure with a superlattice, provided that the wave that goes into the substrate (E_4) is completely absorbed by it.

Based on the conservation of the tangential components of the electromagnetic field, we can obtain a relation for the reflection index (the contribution of reflection from the back side of the substrate is not taken into account):

$$\frac{E_1}{E} = \frac{(N_2 + N_3)(N_1 - N_2) + \exp(\frac{2\pi i}{\lambda} N_2 \cdot 2d) \cdot (N_2 - N_3)(N_1 + N_2)}{(N_2 + N_3)(N_1 + N_2) + \exp(\frac{2\pi i}{\lambda} N_2 \cdot 2d) \cdot (N_2 - N_3)(N_1 - N_2)}$$

$$R_1(\lambda) = |E_1/E|^2 \qquad \text{(S8)}$$

Similarly, for transmission one can get the following expression:

$$\frac{E_4}{E} = \frac{\exp(\frac{2\pi i}{\lambda} N_2 \cdot d) \cdot 4N_1 N_2}{(N_2 + N_3)(N_1 + N_2) + \exp(\frac{2\pi i}{\lambda} N_2 \cdot 2d) \cdot (N_2 - N_3)(N_1 - N_2)}$$

$$T_1(\lambda) = |E_4/E|^2 \qquad \text{(S9)}$$

If emission propagates from the side of the substrate, then expressions (S7, S8) will have the following form:

$$\frac{E_1}{E} = \frac{(N_2 + N_1)(N_3 - N_2) + \exp(\frac{2\pi i}{\lambda} N_2 \cdot 2d) \cdot (N_2 - N_1)(N_3 + N_2)}{(N_2 + N_1)(N_3 + N_2) + \exp(\frac{2\pi i}{\lambda} N_2 \cdot 2d) \cdot (N_2 - N_1)(N_3 - N_2)}$$

$$R_2(\lambda) = |E_1/E|^2 \qquad \text{(S10)}$$

$$\frac{E_4}{E} = \frac{\exp(\frac{2\pi i}{\lambda} N_2 \cdot d) \cdot 4N_3N_2}{(N_2 + N_1)(N_3 + N_2) + \exp(\frac{2\pi i}{\lambda} N_2 \cdot 2d) \cdot (N_2 - N_1)(N_3 - N_2)}$$

$$T_2(\lambda) = |E_4/E|^2 \qquad \text{(S11)}$$

The reflection (R_e) and transmittance (T_e) coefficients determined experimentally differ markedly from the values of R_1 and T_1 given by expressions (S8,S9) if the substrate is transparent. In this case, for consistent analysis of experimental data, it is necessary to take into account reflections from the back side of the substrate.

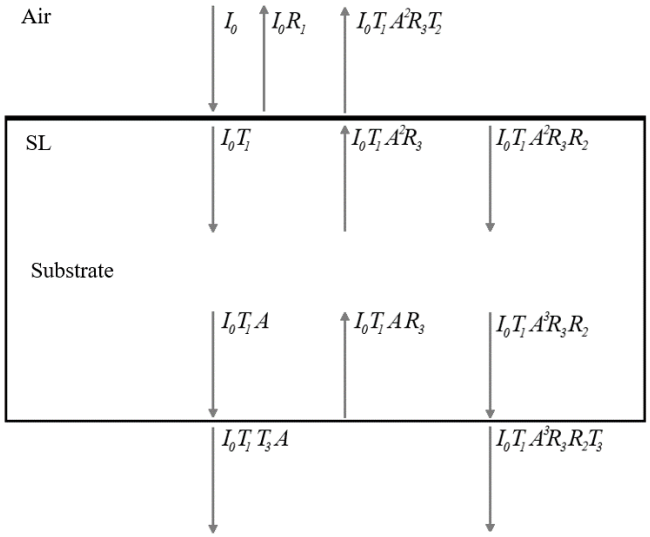

Fig. S4. Diagram showing part of the re-reflection processes of a plane wave in the substrate on which the heterostructure is grown. The given coefficients correspond to the averaging of intensity over interference oscillations over the thickness of the substrate.

A diagram showing part of the re-reflections in the structure on the substrate is shown in Fig. S4. The reflection coefficients R_1 and transmission coefficients T_1 correspond to the coefficients determined by expressions (S8) and (S9), respectively. Reflectance coefficients R_2 and T_2 correspond to the processes of reflection and transmission of light by the heterostructure during light propagation from the substrate side. They are determined by expressions (S10) and (S11), respectively. The coefficients R_3 and T_3 correspond to the reflection and transmission of light from the back side of the substrate. Parameter A reflects the attenuation of light due to its absorption by the substrate during a single passage through it:

$$A = \exp(-\frac{2 \cdot 2\pi}{\lambda} Im[N_3]) \qquad \text{(S12)}$$

All coefficients in Fig. S4 refer to the intensity of the electromagnetic field. To calculate the total reflection coefficient, it is necessary to sum up the contribution from all re-reflections, which will lead to the expression:

$$R_e^{SL} = R_1 + T_1 A^2 R_3 T_2 / (1 - A^2 R_2 R_3) \quad \text{(S13)}$$

This expression is obtained by summing the geometric progression with the denominator $A^2R_2R_3$. Similarly, for transmission the following expression is obtained:

$$T_e^{SL} = T_1 T_3 A / (1 - A^2 R_2 R_3) \quad \text{(S14)}$$

Substituting the refractive and absorption indices of the substrate n and κ calculated at the previous stage in the form $N_3=n+i\kappa$, taking $N_1=1$ as the refractive index of air, and R_e^{SL} and T_e^{SL} from the experimentally measured reflection and transmission spectra of the heterostructure, respectively, and finally taking $N_2 = n_{SL}+i\kappa_{SL}$, we can find the values of the refractive index n_{SL} and absorption index κ_{SL} of the superlattice from the system of equations (S13,S14), see below.

3.2. 500-2000 cm^{-1} range.

In this range it is impossible to use equation (S14) due to the strong absorption of the substrate. Therefore, to estimate $n_{SL}+i\kappa_{SL}$, we used a test function for the permittivity, the real and imaginary parts of which satisfy the Kramers-Kronig relations. Since SL is characterized by a stepped absorption spectrum, for a rough approximation of ε'' we used the simplest "asymmetric resonance" model:

$$\varepsilon''(w) = 0, \quad w \le w_1 \quad \text{(S15)}$$

$$\varepsilon''(w) = A\,\frac{w - w_1}{w_2 - w_1}, \quad w_1 \le w \le w_2 \quad \text{(S16)}$$

$$\varepsilon''(w) = A\,\frac{w_3 - w}{w_3 - w_2}, \quad w_2 \le w \le w_3 \quad \text{(S17)}$$

$$\varepsilon''(w) = 0, \quad w \ge w_3 \quad \text{(S18)}$$

Using the Kramers-Kronig relation, it is easy to show that in this case:

$$\varepsilon'(\Omega) - \varepsilon_\infty = -\frac{C}{\pi(w_2 - w_1)} \cdot$$

$$\cdot\ [(w_1 + \Omega)\cdot ln(w_2 + \Omega) + (w_1 - \Omega)\cdot ln|w_2 - \Omega| - (w_1 + \Omega)\cdot ln(w_1 + \Omega) - (w_1 - \Omega) \cdot ln|(w_1 - \Omega|]$$

$$+\frac{C}{\pi(w_3 - w_2)} \cdot$$

$$\cdot\ [(w_3 + \Omega)\cdot ln(w_3 + \Omega) + (w_3 - \Omega)\cdot ln|w_3 - \Omega| - (w_3 + \Omega)\cdot ln(w_2 + \Omega) - (w_3 - \Omega) \cdot ln|w_2 - \Omega|] \quad \text{(S19)}$$

Note that (S19) contains singular points at which the function is not defined. However, these points are eliminated by passing to the limit. Thus, expressions (S14-S18) allow us to (roughly) simulate the features corresponding to the intersubband transition in the superlattice. A characteristic step is realized if $w_3 - w_2$ significantly exceeds $w_2 - w_1$.

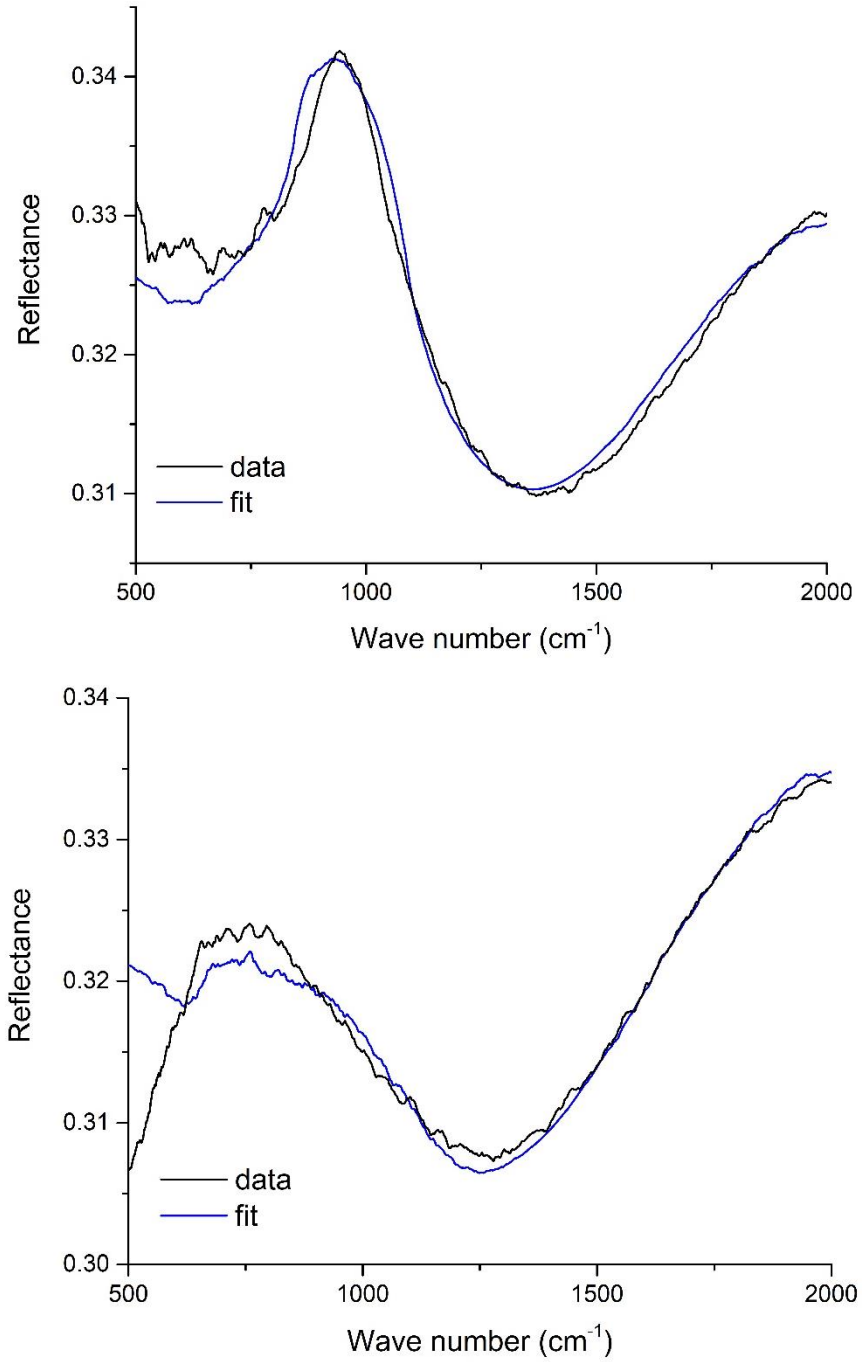

Fig. S5. Results of fitting experimental reflectance spectra (black curve) in the range 500-2000 cm^{-1} based on the complex dielectric function specified by (S15-S19) (blue curve) for temperatures 77 K (top) and 300 K (bottom).

The parameters w_1, w_2, w_3, C, ε_∞ in (S14-S18) were considered as adjustable. The result of the fit for two temperatures is shown in Fig. 5. Next, using the obtained parameter values according to formulas (S15-S19), ε'', ε', n_{SL}, κ_{SL}, were calculated, see Fig. 7. Due to the estimated nature of the calculations for the range 500-2000 cm^{-1}, we did not use continuous cross-linking conditions with more accurate calculations for the range 2000-7000 cm^{-1}.

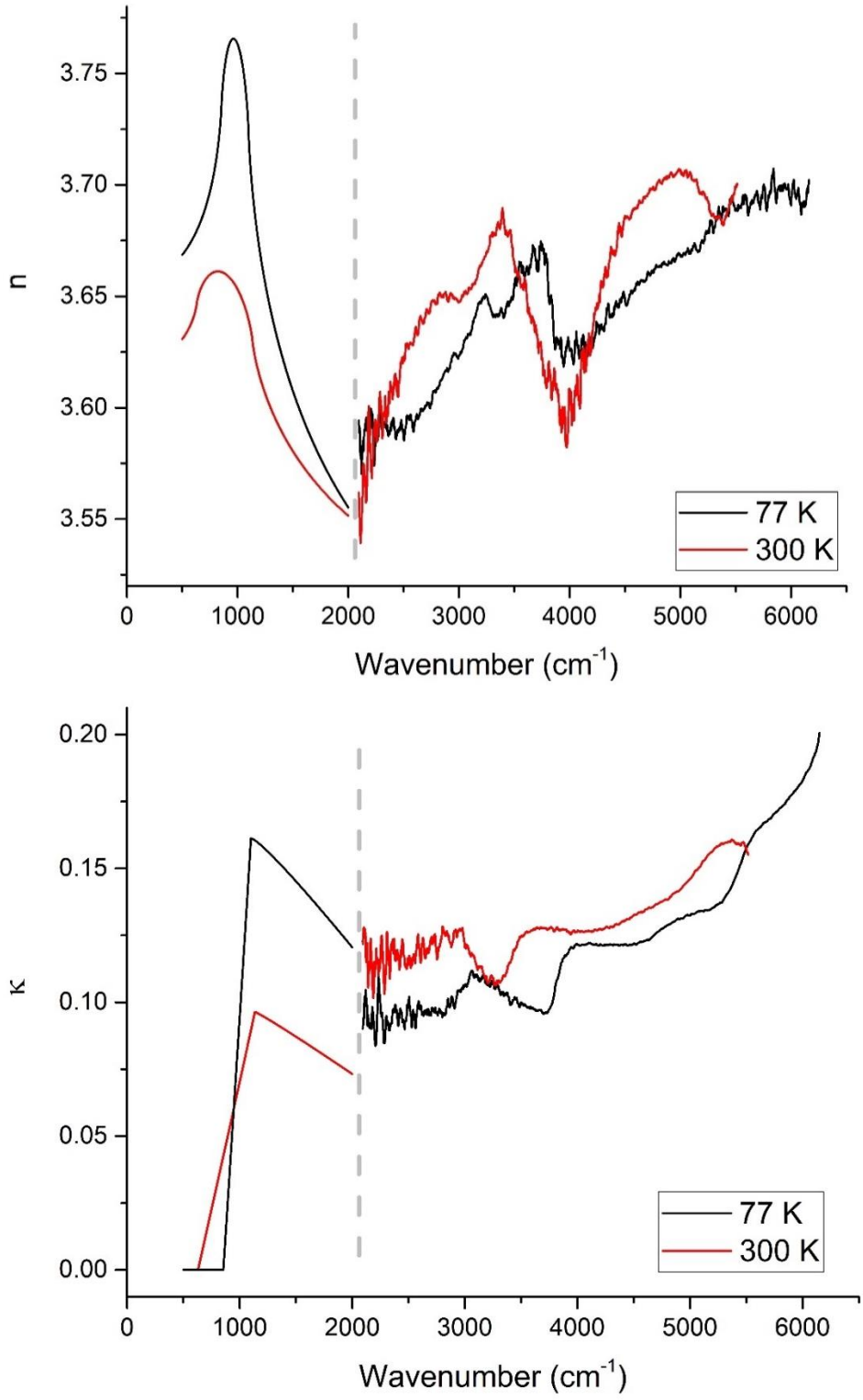

Fig.S6. (top) SL refractive index for temperatures 77 K (black curve) and 300 K (red curve), calculated in the ranges 500-2000 cm^{-1} and 2000-7000 cm^{-1} using the described methods. (bottom) SL absorption index for temperatures 77 K (black curve) and 300 K (red curve), calculated in the ranges 500-2000 cm^{-1} and 2000-7000 cm^{-1} using the described methods.

4. Estimation of energy minibands in a SL.

To estimate the dependence of electron and hole states on the period of InAs/GaSb SL, we used a standard approach, described in detail in [3], based on the formalism of envelope functions in the k·p theory and the effective mass approximation. To obtain minibands of light particles (electrons and light holes) InAs/GaSb SL, where $d = d_1 + d_2$ SL period, d_1 – InAs layer width, d_2 –GaSb layer width, a relationship similar to the Kronig-Penney formula is used:

$$\cos(qd) = \cos(k_1 d_1)\cos(k_2 d_2) - \frac{1}{2}\left(\xi + \frac{1}{\xi}\right)\sin(k_1 d_1)\sin(k_2 d_2) \tag{S20}$$

Here q – superlattice wave vector $(-\pi/d < q \leq \pi/d)$. The bottom of the InAs conduction band is taken as the zero energy point, then the energy of light particles is found from the expressions [3]:

$$\begin{cases} \hbar^2 k_1^2 P = E\left(E + E_g^{InAs}\right) \\ \hbar^2 k_2^2 P = (E - V_s)\left(E - V_s + E_g^{GaSb}\right) \end{cases} \tag{S21}$$

where P is the Kane matrix element [4], $E_g^{InAs} = 0.415$ eV, $E_g^{GaSb} = 0.813$ eV – band gaps of InAs and GaSb, respectively (300 K, for lower temperatures well-known empirical formulas were used), $V_s = 0.96$ eV – energy shift of the bottom of the conduction band of GaSb relative to InAs [3]. The parameter ξ from (S20) is described by the formulas:

$$\xi = \frac{k_1}{k_2}\frac{m_2(E)}{m_1(E)} \tag{S22}$$

$$\begin{cases} \dfrac{1}{m_1(E)} = \dfrac{2P^2}{3}\left(\dfrac{2}{E + E_g^{InAs}}\right) \\ \dfrac{1}{m_2(E)} = \dfrac{2P^2}{3}\left(\dfrac{2}{E + E_g^{InAs} - V_p}\right) \end{cases} \tag{S23}$$

where V_p=0.56 eV – energy shift of the GaSb valence band ceiling relative to InAs [3]. Solving expression (S20) for q=0 and q=π/d minibands of electron and light hole levels were found depending on the superlattice period d.

To obtain minibands of heavy holes, expression (S20) is also used, however (S21, S22) must be replaced with the following expressions:

$$\begin{cases} k_1 = \sqrt{\dfrac{2M_1}{\hbar^2}\left(-E - E_g^{InAs}\right)} \\ k_2 = \sqrt{\dfrac{2M_2}{\hbar^2}\left(-E - E_g^{InAs} + V_p\right)} \end{cases} \tag{S24}$$

$$\xi_{hh} = \frac{k_1}{k_2}\frac{M_2}{M_1} \tag{S25}$$

where $M_1 = 0.57m_e$ and $M_2 = 0.35m_e$ – effective masses of heavy holes in InAs and GaSb, respectively [3].

The above formulas are valid for the wave vector in the superlattice plane $k_\perp = 0$, and also do not take into account spin-orbit splitting.

5. Table

Transition type	Transition energy (edge), estimation, cm^{-1}	Transition energy (edge), experiment, cm^{-1}	Transition energy (maximum), estimation, cm^{-1}	Transition energy (maximum), experiment, cm^{-1}	Energy shift of a maximum 77-300 K, experiment, cm^{-1}
e_1-hh_1	1202	855	1807	1100	34
e_1-hh_2	2936	2853	3541	3063	98
e_1-lh_1	3234	3691	3905	3976	437
e_2-hh_1	4236	4591	4840	4918	425
e_1-E_v^{InAs}	5062	5305	5663	5616	400

Table S1. Estimated energies of transitions, their comparison with experimental values at a temperature of 77 K and the shift of transitions with increasing temperature to 300 K.

[1] Mishra, P., Pandey, Rakesh. K., Kumari, S., Pandey, A., Dalal, S., Sankarasubramanian, R., Channagiri, S., Jangir, S. K., Raman, R., Srinivasan, T. & Rao, D. V. S. Interface engineered MBE grown InAs/GaSb based type-II superlattice heterostructures. Journal of Alloys and Compounds 889, 161692 (2021)

[2] Bolkhovityanov Yu B, Pchelyakov O P, Chikichev S I "Silicon-germanium epilayers: physical fundamentals of growing strained and fully relaxed heterostructures" Physics-Uspekhi 44 655–680 (2001)

[3] Bastard G., Brum J. A. Electronic States in Semiconductor Heterostructures, IEEE Journal of Quantum Electronics. – 1986. – № QE-22. – С. 1625-1644.

[4] Y. Livneh, P. C. Klipstein, O. Klin, N. Snapi, S. Grossman, A. Glozman, and E. Weiss, k·p model for the energy dispersions and absorption spectra of InAs/GaSb type-II superlattices, Phys. Rev. B 86, 235311 (2012)